

Ejecta and the Late Stages of Stellar Evolution

T. M. Gledhill

*Centre for Astrophysics Research, Science and Technology Research
Centre, University of Hertfordshire, Hatfield, AL10 9AB, UK.*

Abstract. The late stages of stellar evolution are characterised by prodigious mass-loss, particularly on the Asymptotic Giant Branch (AGB), resulting in the build up of a circumstellar envelope of gas and dust. In this way, the majority of stars ($\sim 0.8 M_{\odot} < M < \sim 8 M_{\odot}$) will have shed their excess mass by the end of the AGB, allowing them to evolve to hotter temperatures to become the central stars of planetary nebulae (PN). With the expulsion of so much dust into the circumstellar environment, polarization (and polarimetry) becomes a key technique in the study of these objects. At wavelengths shortwards of $5 \mu\text{m}$, AGB and post-AGB objects (those in transition to the PN phase are often termed proto-PN) are seen predominantly by dust-scattered light, and are therefore polarized. Imaging polarimetry may be used to investigate the geometry of the dust shells, the distribution of dust therein (and hence the mass-loss rate evolution on the AGB) and also the nature of the scattering particles themselves (the dust grains). A particularly enduring puzzle concerns the origin of the complex structures seen in PN, which originate from what are presumed to be spherically symmetric outflows on the AGB. Polarimetry is the natural tool with which to search for and investigate the origin of asymmetric structure, such as bipolar outflows, which reveal themselves in the form of significant net linear polarization. At wavelengths longer than $5 \mu\text{m}$, thermal emission from warm (150 K) dust prevails. This too may be polarized, if the grains are non-spherical and aligned, for example by a magnetic field. The possible role of magnetic fields in driving and collimating asymmetric outflows from evolved stars, in the form of magnetised winds, has received recent attention, and a number of theoretical models have been proposed. The ability of polarimetry to detect these fields and to determine their structure will offer vital observational tests for the models. An alternative approach to determining field configurations and strengths is the use of polarimetric imaging of maser emission at radio wavelengths. The use of polarimetry in studies of evolved stars and their ejecta, over a wide range of wavelengths and spatial resolutions will be reviewed.

1. Mass-loss from Evolved Stars

Imaging polarimetry has been used extensively to investigate the dust enshrouded environments of young stars (these Proceedings). Sources are often deeply embedded so that the only emergent light in the optical and near-IR wavelength ranges is that which is scattered into our line of sight by dust grains. This results in reflection nebulae which can be highly polarized. Evolved stars are also dusty objects due to the intense radiation-driven winds that occur during the AGB phase. Mass-loss increases with time spent on the AGB ($\sim 10^6$ yr) as the core mass and luminosity increase, reaching a peak of up to $10^{-4} M_{\odot} \text{ yr}^{-1}$ at the tip of the AGB. The optical depth due to dust extinction therefore increases along

the AGB and, in the last phase before cessation of mass-loss, the object may be completely obscured by the dusty envelope (e.g. Habing 1996 for a review).

At the end of the AGB, the mass-loss rate drops abruptly to below $\sim 10^{-7}$ solar masses per year (Blöcker 1995) and the star is surrounded by a detached slowly expanding ($10\text{-}20 \text{ km s}^{-1}$) circumstellar envelope (CSE). In this immediate post-AGB phase, the star has yet to become hot enough to photoionise the gas, so that emission from dust grains and molecular gas generally dominates. However, some post-AGB objects do power fast, highly collimated winds capable of shock exciting the surrounding material. A notable example is OH 231.8+4.2 with its $> 400 \text{ km s}^{-1}$ molecular outflow (Alcolea et al. 2001). Such objects may result from tidal interaction of the mass-losing star with a binary companion (e.g. Soker 2002).

2. Roles for Polarimetry

2.1. Scattered Light

Although there is evidence that large ($> 1 \mu\text{m}$) grains do exist around evolved stars (e.g. Jura, Turner & Balm 1997), there is also strong evidence (from polarimetric observations and from model fits to mid-IR imaging) for a large population of small ($\sim 0.2 \mu\text{m}$) grains in the CSEs of post-AGB objects (Gledhill et al. 2001; Gledhill & Yates 2003). At wavelengths less than $\sim 5 \mu\text{m}$, for sub- μm grain sizes, scattering is the predominant emission mechanism and the CSE is then visible in polarized light. In cases where the central star is visible, the direct flux is unpolarized, so that in polarized light the star is suppressed, allowing the CSE to be seen more easily. Imaging polarimetry is then a powerful technique for the detection of scattering envelopes around AGB and post-AGB stars and for the investigation of their structure (subject to angular resolution constraints).

Polarimetric information can also be used to place limits on grain properties, such as the grain size distribution. This is especially the case when observations are obtained at several wavelengths and where other constraints on grain composition are available (e.g. from a general knowledge of the CSE chemistry or from specific observations of dust emission features).

Recent imaging surveys (e.g. Ueta et al. 2000) and polarimetric imaging surveys (Gledhill, Yates, & Richards 2001) indicate that the CSE in the post-AGB phase is in almost all cases asymmetric to some degree (usually axisymmetric). Polarimetry is a natural tracer of asymmetry and is sensitive to non-isotropic illumination. Even when the asymmetric region is not spatially resolved, a net polarization signature will be observed.

2.2. Thermal Emission

At wavelengths longwards of $\sim 5 \mu\text{m}$ thermal emission from warm dust in the CSE is usually seen. In the post-AGB phase, where the detached CSE is expanding away from the star, the dust temperature at the inner edge of the envelope is typically $\sim 150\text{K}$, and a dust thermal continuum peaking in the wavelength range $25\text{-}30 \mu\text{m}$ range is seen. Polarization of the thermal continuum, or of dust features, indicates alignment of non-spherical dust grains. If the alignment mechanism is assumed to be magnetic relaxation (Aitken, these Proceedings) then

polarimetric imaging of the thermal emission provides a technique for detecting and determining the configuration of magnetic fields around evolved stars. This has a strong bearing on the origin of axisymmetry in these objects, since mechanisms have been proposed for the generation of magnetically collimated outflows (Matt et al. 2000; Blackman et al. 2001).

2.3. Maser Emission

The cool molecular envelopes of AGB stars, and to a lesser extent post-AGB stars, support maser emission from several species, including OH, SiO and H₂O. SiO masers are found just above the stellar atmosphere, H₂O masers up to 10¹⁵ cm, OH main line masers (1667 and 1665 MHz) between 10¹⁵ and 10¹⁶ cm and OH 1612 MHz emission at $\sim 10^{16}$ cm radius from the star. Each species therefore probes a specific environment from the dust formation region (SiO) to the CSE (OH). As well as providing a means to probe the gas distribution and kinematics around the star on fine spatial scales (from mas upwards), the presence of a magnetic field will lead to Zeeman splitting of the maser lines and the possibility of determining the field strength and structure.

3. Early Polarimetric Work

The earliest polarimetric observations of evolved stars were made as part of Hiltner's work on ISM polarization (e.g. Hiltner 1951) using a photoelectric photometer and a piece of polaroid. This was followed by work in the 1960s by Serkowski using the 20 inch (0.66 m) refractor at Belgrade University and a similar setup with photometer and polaroid. Forbes (1967) obtained some of the first IR observations, with a liquid N cooled PbS photopolarimeter at the Catalina 66 inch (1.7 m) using a polaroid sheet at J, H and K and a wire grid at L band. He measured 4-5 per cent polarization for NML Cyg (a supergiant) but concluded that it was of interstellar origin. All of these observations used nearby bright stars (some of which were evolved stars) as a probe of the intervening ISM polarization, rather than being an investigation of the nature of the object itself.

The first imaging polarimetry of a post-AGB object was obtained by Schmidt, Angel & Beaver (1978) in an optical study of AFGL 2688 (the Egg Nebula) and M1-92, using a 200 element digicon detector and Pockels cell polarimeter (Figure 1). The high degree of linear polarization in this object had already been remarked upon by Ney et al. (1975) and Michalsky et al. (1976) but the imaging observations revealed a centrosymmetric scattering pattern with degrees of polarization exceeding 50% in the bipolar lobes in the case of AFGL 2688. Zuckerman et al. (1976) had suggested that AFGL 2688 was a PN precursor, although Cohen & Kuhl (1977) proposed a pre-main sequence status. Circular polarization of 0.6 per cent has also been observed in AFGL 2688 between 400 and 800 nm (Michalsky et al. 1976) and attributed to either scattering or transmission through magnetically aligned dust grains. Further optical imaging polarimetric studies of nebulae associated with evolved stars were published in the late 70s and early 80s by the Durham group (Eta Carinae: Warren-Smith et al. 1979; The Boomerang Nebula: Taylor & Scarrott 1980; M2-9: King et al. 1981; The Red Rectangle: Perkins et al. 1981).

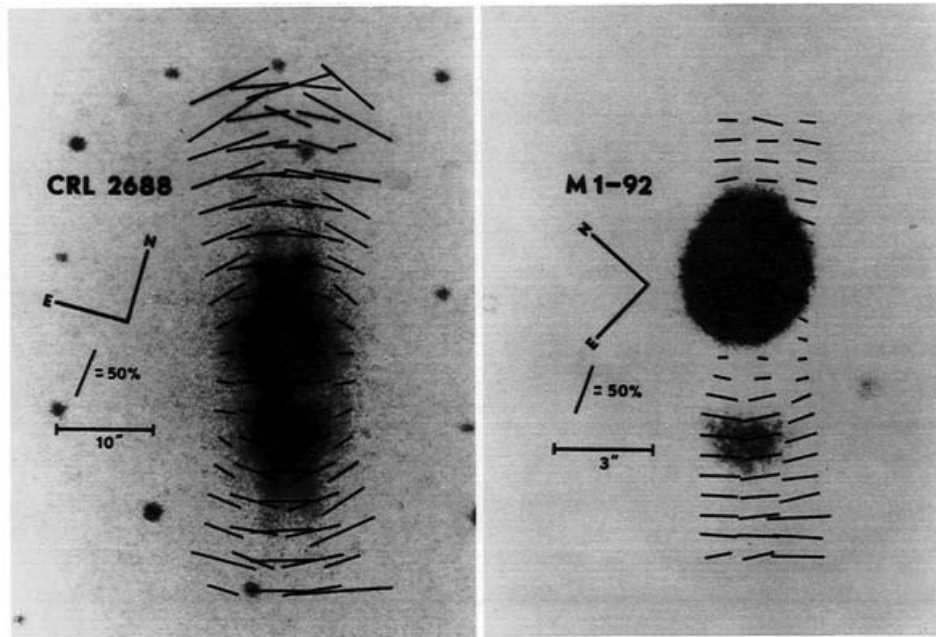


Figure 1. Imaging polarimetry of AFGL 2688 and M 1-92, superimposed on photographs of the objects, from Schmidt et al. (1978).

4. Polarimetry as a Survey Tool

Scattering in an asymmetric environment, such as a dust disc or flattened shell, will result in a net polarization, even if the region of asymmetry is not resolved. In aperture near-IR polarimetric observations, McCall & Hough (1980) surveyed 29 ‘cool stars’ and detected a correlation between degree of polarization and IR colour index, such that highly polarized stars also had a large IR excess. This was early evidence suggesting that the obscuration around evolved stars is asymmetric. It is now known from imaging and imaging polarimetric studies that many post-AGB objects possess asymmetric outflows and dusty discs.

In a more extensive survey, Johnson & Jones (1991) use aperture polarimetry at optical and near-IR wavelengths to investigate the development of asymmetry in 42 objects in a range of evolutionary stages from RGB to PN. They find that aspherical outflow is a common feature in evolved stars and that the degree of polarization is correlated with the IR excess and hence with the mass-loss rate, peaking at the end of the AGB.

A spectropolarimetric survey by Trammell et al. (1994) was the first to concentrate specifically on objects in transition between the AGB and PN phases. They found that aspherical structure appears very early on in the AGB-PN transition and that there is no obvious correlation between the degree of polarization (and hence degree of axisymmetry) and the O/C chemistry of the object (also noted by McCall & Hough 1980).

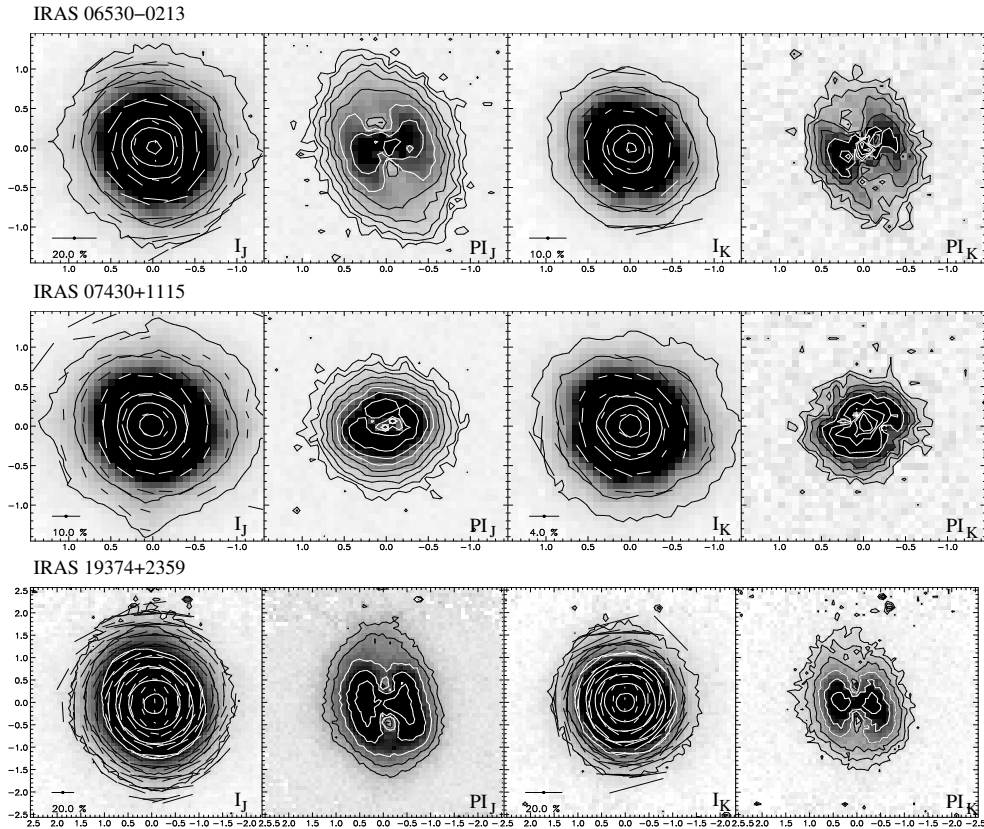


Figure 2. Imaging polarimetry results from Gledhill (2004) for objects that show a detached shell morphology in polarized light. Total intensity (I) images are superimposed with polarization vectors alongside polarized intensity (PI) images for both J and K wavebands. Although in the I images, the objects appear as bright, slightly extended, point sources, in the PI images, the star effectively disappears revealing the detached shell nature of the CSE.

5. Imaging Circumstellar Envelopes in Scattered Light

5.1. Ground-based Surveys

Ground-based imaging polarimetry can be used as a fast and efficient technique for the detection of extended scattering envelopes around post-AGB sources, allowing the separation of the polarized CSE from the unpolarized PSF. This overcomes the problem of imaging faint material close to a bright star, which can be particularly acute in the case of nebulae associated with very bright post-AGB stars. In the optical survey of Ueta et al. (2000), the average star-to-nebula ratio was $\sim 10^4$ for objects where the star is visible, necessitating a large dynamic range in order to image the nebulosity. Also, in the post-AGB phase, the detached CSE is expected to have an inner radius $\sim 10^{16}$ cm (e.g. Steffen et al. 1998) or 0.66 arcsec at 1 kpc, so that, for ground-based observations, the nebulosity may be hidden under the wings of the bright central PSF. Imaging polarimetry provides a means to overcome these problems, and in the near-

IR survey of Gledhill et al. (2001), scattering envelopes were detected around 16 candidate post-AGB sources. This survey has recently been extended to a further 20 objects (Gledhill 2004). The CSE morphologies range from mildly elliptical shells (Figure 2), to highly bipolar nebulae. A high proportion of objects show large degrees of linear polarization with aligned vector patterns, but no obvious structure in polarized flux images. These objects may be unresolved bipolar nebulae. In all cases, there is clear evidence for axisymmetry. The division between shells and bipolars appears to be due to the amount of dust in the circumstellar environment, with the former being optically thin and the latter optically thick. Scattering models reproduce these morphologies using a simple axisymmetric density model for the CSE (Gledhill 2004).

5.2. HST Imaging Polarimetry

The limited spatial resolution of ground-based observations, combined with the high optical depths of the central regions, makes imaging polarimetry in the near-IR with NICMOS on HST a powerful probe of post-AGB CSEs. Sahai et al. (1998) present NICMOS imaging polarimetry of AFGL 2688 (the Egg Nebula) at $2 \mu\text{m}$, showing a centrosymmetric vector pattern indicating an illuminating source located in the dust lane, as seen in earlier ground-based observations (e.g. Schmidt et al. 1978). However, the improved spatial resolution of the NICMOS observations reveals the extremely high degrees of polarization, of 70-80 per cent, along the edges of the bicones and in the ‘searchlight beams’. This places strong constraints on the sizes of the dust grains responsible for the scattering and polarization at $2 \mu\text{m}$, with calculations based on spherical grains indicating that they must be smaller than $0.2 \mu\text{m}$ in radius. Similarly high degrees of linear polarization have been found in other bipolar post-AGB nebulae, such as IRAS 17150-3224 (Figure 3), again using NICMOS (Su et al. 2003). In ground-based observations, the degrees of polarization are usually lower as regions with differing vector orientations are smoothed into one another by the seeing profile. This illustrates the need for spatially resolved imaging polarimetry if the true intrinsic degree of polarization is to be measured.

High spatial resolution imaging polarimetry also offers the opportunity to investigate detailed structure in polarization patterns and to locate hidden illuminating sources. Weintraub et al. (2000) use the NICMOS polarimetry of Sahai et al. (1998) to accurately determine the location of the illuminating source in the central dusty lane of AFGL 2688, showing it to lie ~ 0.55 arcsec from the bright IR peak. At a distance of 1 kpc, this corresponds to 550 AU on the sky or, assuming the bipolar axis is inclined at 15° to the plane of the sky and that both sources lie in the equatorial plane, ~ 1000 AU. They conclude that although the two components may both reside within the dust disc and, hence, form a binary system, the separation is too great for the presence of the companion to account for the bipolar structure of the nebula. These authors also find a strong point-symmetric structure in the nebulosity and in the degree of polarization, centred on this hidden illuminating source. Similar point-symmetric structures are seen in IRAS 17150-3224 and 17441-2411 (Su et al. 2003) and are suggestive of precessing collimated outflows (Figure 3). Point-symmetry is also common in young planetary nebulae (Sahai & Trauger 1998).

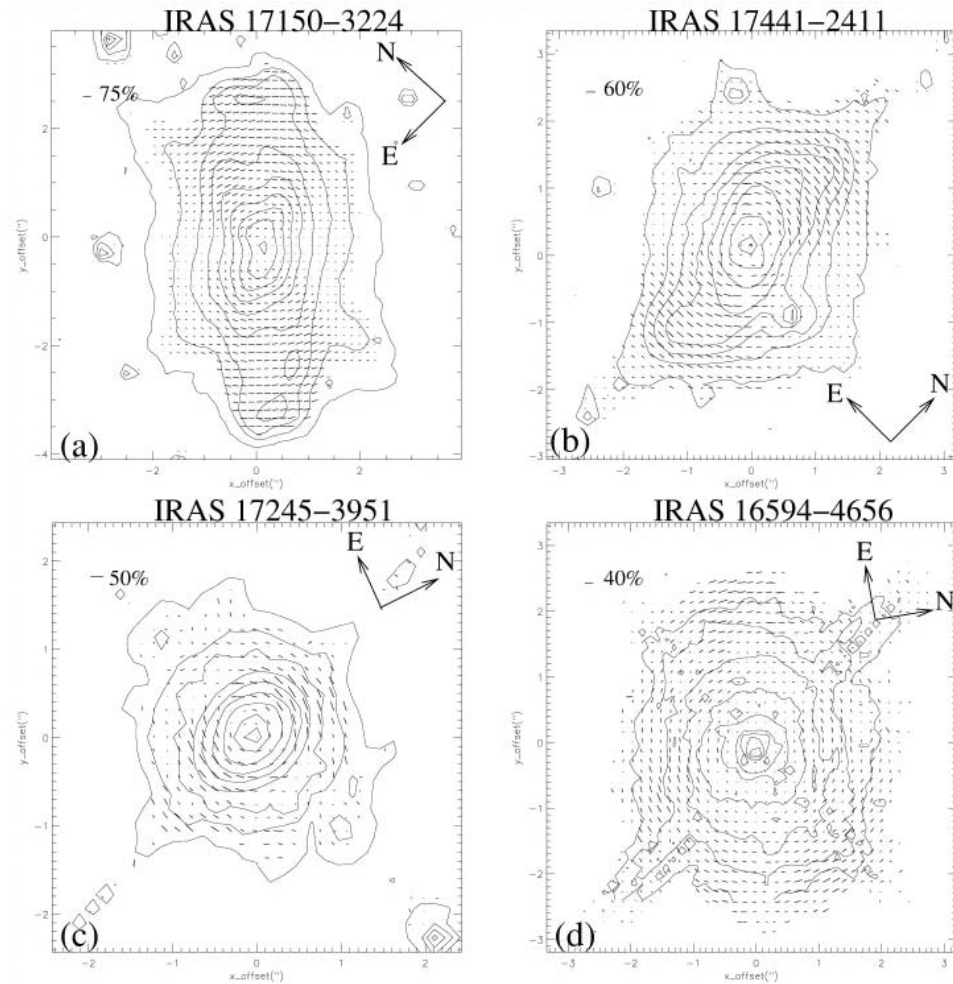


Figure 3. NICMOS imaging polarimetry of four proto-PN at $2 \mu\text{m}$ from Su et al. 2003.

6. Axisymmetry and Magnetic Fields

Surveys using high spatial resolution and polarimetric imaging techniques are suggesting that the presence of asymmetric outflow may be a ubiquitous phenomenon by the post-AGB stage. The questions then are how and when does this asymmetry arise? Models tend to invoke one of two mechanisms: binary action (e.g. Soker & Rappaport 2000) or magnetic collimation (e.g. Matt et al. 2000). It may turn out to be the case that both are required and that one leads naturally to the other. An apparent problem with the binary star hypothesis is that if all post-AGB outflows are asymmetric then the required binary frequency is higher than currently suggested by observation (Bond 2000). However, this may turn out to be less acute if orbiting planets can induce asymmetric outflow (Soker 2001) and/or there is an observational selection effect operating by which bipolar post-AGB objects are more likely to be observed (e.g. they evolve

more slowly than less asymmetric objects: Zijlstra et al. 2001). In addition to the shaping problem, it appears that many post-AGB objects have too much momentum in the outflow to be explained by radiative acceleration from the central luminosity alone, even assuming multiple scattering (Bujarrabal et al. 2001). The idea that magnetic fields may play a role in the collimation and acceleration of outflows in the late AGB/post-AGB phase is then attractive in that it may present a single star evolutionary path to aspherical PN. Although a dynamo mechanism for the generation of a field, with sufficient strength to collimate bipolar outflows, has been proposed (Blackman et al. 2001), there is still little conclusive evidence that B-fields exist in the CSEs of post-AGB objects with sufficient energy density to collimate an outflow. As mentioned in Section 2, polarimetry of thermal dust emission and maser emission may reveal the presence of such fields if they exist.

7. Polarized Thermal Emission

Polarimetry of the thermal continuum from both warm and cool dust (i.e. in the mid-IR through to sub-mm) has been used extensively to map the magnetic field structure of star forming clouds (e.g. Aitken et al. 1997 and review by Matthews, these proceedings). Its use as a tool to investigate the CSEs of post-AGB stars is much less advanced, largely due to the much smaller polarizations expected (and hence greater polarimetric precision required) and the spatial resolution constraints of imaging at these longer wavelengths.

The inner regions of the CSE in the post-AGB phase radiate predominantly in the mid-IR, with dust temperatures $\sim 150 - 200$ K, so that mid-IR polarimetry should provide a powerful means to detect and study any B-fields in these regions. However, the availability of mid-IR polarimeters with sufficient precision to detect polarizations of 1 or 2 per cent is poor. Aitken et al. (1995), using a private instrument (NIMPOL), detected polarization at $12.5 \mu\text{m}$ of between 3 and 4 per cent in the shell of Eta Carinae (a very high mass LBV whose CSE results from an outburst in 1843). Polarization angles are orthogonal to those seen at optical wavelengths (Warren-Smith et al. 1979) so that the polarizing mechanism is likely to be emission by aligned non-spherical grains. Aitken et al. (1995) suggest that the star may have exploded into an already magnetised circumstellar torus.

Observations at far-IR wavelengths provide the opportunity to probe the cooler outer regions of post-AGB outflows. The problem here is that sub-mm observations currently have sufficient spatial resolution to image only the most extended objects, on a scale of tens of arcseconds, whereas most CSEs subtend only 1 or 2 arcseconds. Greaves (2002) presents $850 \mu\text{m}$ polarimetry of AFGL 2688 (the Egg Nebula) and NGC 7027 (a dusty PN) and finds evidence for a toroidal magnetic field around NGC 7027.

8. Maser Mapping and Polarimetry

SiO masers lie between the stellar photosphere and the dust formation zone, a region which is often pulsationally unstable and thought to be instrumental in the initiation of a dust driven wind. Diamond & Kembal (2003) obtained

VLBA observations of the 43 GHz SiO maser transition around the Mira variable TX Cam, over the full 557 day pulsational cycle. The SiO masers trace a dominant expansion in the envelope, as well as local inflow and outflow motions. There is also evidence for significant deviation from spherical symmetry in the morphology and evolution of the SiO emission.

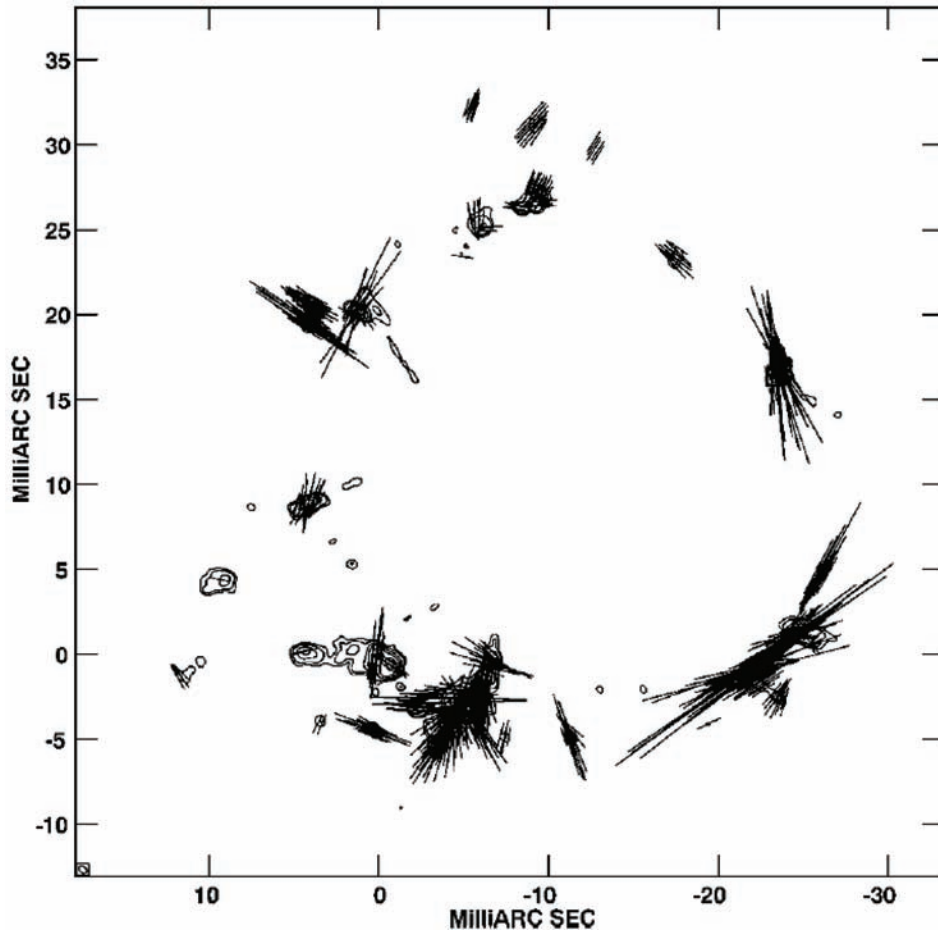


Figure 4. Linearly polarized SiO masers in the shell around TX Cam, from Kemball & Diamond (1997).

SiO masers also provide the opportunity to determine the B-field configuration in the extended atmospheres of late-type stars at very high (milliarcsecond) spatial resolution. Kemball & Diamond (1997) derive a mean magnetic field strength of $B \sec \theta \sim 5 - 10$ G (where θ is the angle between the field and the line of sight). Interpretation of the field topology and discrimination between radial, toroidal and poloidal models is difficult due to intricacies concerning the orientation of the linear polarization relative to B depending on θ , but Kemball and Diamond conclude that there is an ordered field over a significant portion of the maser shell, with a poloidal configuration being consistent with the observations (Figure 4).

Hydroxyl (OH) masers occur in the CSEs of late-type stars, at radii of $\sim 10^{16}$ cm from the star. The maser transitions are often seen with a red- and blue-shifted peak (relative to the stellar velocity), indicating an expanding shell of gas (Habing 1996). Interferometric observations using the MERLIN array allow mapping of the distribution and kinematics of OH masers on a spatial scale of ~ 0.2 arcsec and with a velocity resolution of 0.35 km s^{-1} . This technique was used to image the thick maser shell around the possible hypergiant HD 179821 (Gledhill, Yates & Richards 2001), showing it to be expanding at 30 km s^{-1} . The shell appears incomplete and may have been disrupted by a more recent outflow.

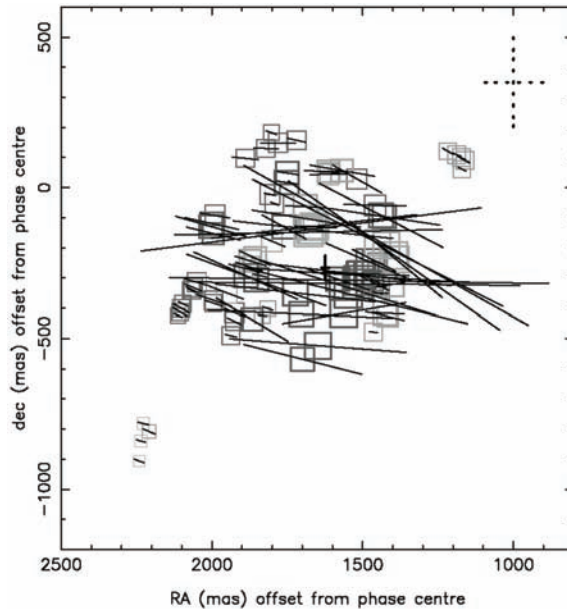


Figure 5. Linearly polarized OH maser components at 1612 MHz in the equatorial dust disc of the bipolar post-AGB object IRAS 18271-1431 (OH17.7-2.0). Bains et al. (2003).

Detection and mapping of magnetic fields in the CSE is possible using Zeeman splitting of the OH maser lines. Bains et al. (2003) present spectral line polarimetry at 1612 and 1667 MHz of the dusty post-AGB object IRAS 18276-1431 (OH17.7-2.0) and detect a fully resolved Zeeman sigma component at each frequency leading to an estimate of the magnetic field strength of 4.6 mG and 2.5 mG at 1612 and 1667 MHz respectively. The polarization mapping suggests a field with a stretched dipole structure (Figure 5) which, when compared with near-IR polarimetric imaging, shows the masers to lie in an optically thick equatorial disc, oriented perpendicular to a bipolar outflow seen in scattered light. Bains et al. (2003) suggest that the field may have played a role in collimation of the outflow.

9. Summary

Imaging polarimetry at optical and near-IR wavelengths provides a powerful technique with which to detect the CSEs of stars in the post-AGB phase in scattered light. Surveys completed using 4-m telescopes have shown that the CSE structure is nearly always axisymmetric to some degree and are allowing us to characterise the degree of axisymmetry. HST imaging polarimetry with NICMOS has demonstrated the benefits of increased spatial resolution in determining detailed structure, revealing point-symmetries and imaging the central optically thick disc region of bipolar post-AGB objects. The availability of polarimetric capabilities on 8-m telescopes is essential if we are to further our understanding of these objects through routine investigations on the required spatial scales.

Although the range of scenarios that lead to the morphological diversity observed in proto-PN and PN is not well understood, the possible role of the stellar magnetic field cannot be ruled out. In order to test models invoking magnetic collimation of outflows, it is imperative to try to detect dynamically significant B-fields around stars in the AGB and post-AGB phases. Polarimetric imaging of thermal dust emission and interferometric polarimetry of Zeeman-split maser lines offer this possibility. In the case of maser polarimetry there are already indications that B-fields can play a role in outflow shaping. Imaging polarimetry of dust emission is currently hampered by the scarcity of polarimeters in the mid-IR (where most energy is radiated by the post-AGB CSE) and by limitations of spatial resolution at longer wavelengths. This situation is only likely to change with the availability of accurate (dual beam) mid-IR polarimeters on 8-m telescopes and the advent of sub-mm interferometers with polarimetry.

References

- Aitken D.K., Smith C.H., Moore T.J.T., Roche P.F., Fujiyoshi T., & Wright C.M. 1997, *MNRAS*, 286, 85
- Aitken D.K., Smith C.H., Moore T.J.T., Roche P.F., Puetter R.C., & Pina R.K. 1995, *MNRAS*, 273, 354
- Alcolea J., Bujarrabal V., Sánchez-Contreras C., Neri R., & Zweigle J. 2001, *A&A*, 373, 932
- Bains I., Gledhill T.M., Yates J.A., & Richards A.M.S. 2003, *MNRAS*, 338, 287
- Blackman E.G., Frank A., Markiel J.A., Thomas J.H., & van Horn, H.M. 2001, *Nature*, 409, 485
- Bloeker T. 1995, *A&A*, 299, 755 Bond H., 2000, in *ASP Conf. Ser.* Vol. 199, *Asymmetrical Planetary Nebulae II*, Ed. J.H.Kastner, N.Soker and S.Rappaport, 115
- Bujarrabal V., Castro-Carrizo A., & Alcolea J., Sánchez-Contreras C. 2001, *A&A*, 377, 868
- Cohen M., & Kuhl L.V. 1977, *ApJ*, 213, 79
- Diamond P.J., & Kembell A.J. 2003, *ApJ*, 599, 1372
- Forbes F.F. 1967, *ApJ*, 147, 1226

- Gledhill T.M., Chrysostomou A., Hough J.H., & Yates J.A. 2001, MNRAS, 322, 321
- Gledhill T.M., Yates J.A., & Richards A.M.S. 2001, MNRAS, 328, 301
- Gledhill T.M., & Yates J.A. 2003, MNRAS, 343, 880
- Gledhill T.M. 2004, MNRAS *submitted*
- Greaves J.S. 2002, A&A, 392, L1
- Habing H.J. 1996, A&AR, 7, 97
- Hiltner W.A. 1951, ApJ, 114, 241
- Johnson J.J., & Jones T.J. 1991, AJ, 101, 1735
- Jura M., Turner J., & Balm S.P. 1997, ApJ, 474, 741
- Kemball A.J., & Diamond P.J. 1997, ApJ, 481, L111
- King D.J., Perkins H.G., Scarrott S.M., & Taylor K.N.R. 1981, MNRAS, 196, 45
- Matt S., Balick B., Winglee R., & Goodson A. 2000, ApJ, 545, 965
- McCall A., & Hough J.H. 1980, A&AS, 42, 141
- Michalsky J.J., Stokes R.A., & Ekstrom P.A. 1976, ApJ, 203, L43
- Ney E.P., Merrill K.M., Becklin E.E., Neugebauer G., & Wynn-Williams C.G. 1975, ApJ, 198, L129
- Perkins H.G., Scarrott S.M., Murdin P., & Bingham R.G. 1981, MNRAS, 196, 635
- Sahai R., et al. 1998, ApJ, 492, L163
- Sahai R., & Trauger J.T. 1998, AJ, 116, 1357
- Schmidt G.D., Angel J.R.P., & Beaver E.A. 1978, ApJ, 219, 477
- Soker N., & Rapport S. 2000, ApJ, 538, 241
- Soker N. 2001, MNRAS, 324, 699
- Soker N. 2002, MNRAS, 330, 481
- Steffen M., Szczerba R., & Schoenberner D. 1998, A&A, 337, 149
- Su K.Y.L., Hrivnak B.J., Kwok S., & Sahai R. 2003, AJ, 126, 848
- Taylor K.N.R., & Scarrott S.M. 1980, MNRAS, 193, 321
- Trammell S.R., Dinerstein H.L., & Goodrich R.W. 1994, AJ, 108, 984
- Ueta T., Meixner M., & Bobrowsky M. 2000, ApJ, 528, 861
- Warren-Smith R.F., Scarrott S.M., Murdin P., & Bingham R.G. 1979, MNRAS, 187, 761
- Weintraub D.A., Kastner J.H., Hines D.C., & Sahai R. 2000, ApJ, 531, 401
- Zijlstra A.A., et al. 2001, MNRAS, 322, 280
- Zuckerman B., Gilra D.P., Turner B.E., Morris M., & Palmer P. 1976, ApJ, 205, L15